Available online at www.sciencedirect.com
SCIENCE DIRECT
Journal of Structural Biology 152 (2005) 221–228
Journal of Structural Biology
www.elsevier.com/locate/yjsbi

Architecture of the native photosynthetic apparatus of *Phaeospirillum molischianum*

Rui Pedro Gonçalves [a], Alain Bernadac [b], James N. Sturgis [b], Simon Scheuring [a,*]

[a] *Institut Curie, UMR-CNRS 168, 11 rue Pierre et Marie Curie, 75231 Paris Cedex 05, France*
[b] *UPR-9027 LISM, IBSM, CNRS, 31 Chemin Joseph Aiguier, 13402 Marseille Cedex 20, France*

Received 16 August 2005; received in revised form 29 September 2005; accepted 13 October 2005
Available online 18 November 2005

Abstract

The ubiquity and importance of photosynthetic organisms in nature has made the molecular mechanisms of photosynthesis a widely studied subject at both structural and functional levels. A current challenge is to understand the supramolecular assembly of the proteins involved in photosynthesis in native membranes. We have used atomic force microscopy to study the architecture of the photosynthetic apparatus and analyze the structure of single molecules in chromatophores of *Phaeospirillum molischianum*. Core complexes are formed by the reaction center enclosed by an elliptical light harvesting complex 1. LH2 are octameric rings, assembled either with cores or in hexagonally packed LH2 antenna domains. The symmetry mismatch caused by octameric LH2 packing in a hexagonal lattice, that could be avoided in a square lattice, suggests lipophobic effects rather than specific inter-molecular interactions drive protein organization. The core and LH2 complexes are organized to form a supramolecular assembly reminiscent to that found in *Rhodospirillum photometricum*, and very different from that observed in *Rhodobacter sphaeroides*, *Rb. blasticus*, and *Blastochloris viridis*.

Keywords: AFM; Bacterial photosynthesis; Membrane proteins; Native membrane; Light harvesting

1. Introduction

Photosynthetic bacteria provide an ideal experimental system for the description of assembly and organization of membrane systems. In addition to the wealth of information from biochemistry, molecular biology and spectroscopy, structural data have advanced our understanding of the individual components of the bacterial photosynthetic apparatus and have provided models for its function. The peripheral antenna light harvesting 2 (LH2) complexes initially trap the light energy and this is transferred to LH1 complexes, which are closely associated with the reaction center (RC). The subsequent photon induced charge separation in the RC initiates a cyclic electron transport and the formation of an electrochemical proton gradient across the membrane by the cytochrome bc_1 complex. Finally, the proton gradient is used by the ATP synthase to form ATP (for review see (Hu et al., 2002)).

X-ray crystallography has provided high-resolution structures of most components of the photosynthetic apparatus. High-resolution LH2 structures have been obtained from both *Rhodopseudomonas* (*Rps.*) *acidophila* and *Phaeospirillum* (*Phsp.*) *molischianum*, the species we have studied here. The first reveals a nonameric ring structure (McDermott et al., 1995; Papiz et al., 2003), whereas the second reveals an octamer (Koepke et al., 1996). Each subunit is formed by a heterodimer of α- and β-polypeptides, each polypeptide containing a single membrane spanning α-helix. A recent study of native membranes shows that there is some natural variability of LH2 stoichiometry around the predominant nonameric architecture in native membranes of *Rhodospirillum* (*Rsp.*) *photometricum* (Scheuring et al., 2004a). Structures of the isolated RC from *Blastochloris* (*Blc.*) *viridis* and *Rhodobacter*

* Corresponding author. Fax: +33 1 40510636.
E-mail address: simon.scheuring@curie.fr (S. Scheuring).

1047-8477/$ - see front matter © 2005 Elsevier Inc. All rights reserved.
doi:10.1016/j.jsb.2005.10.002

(*Rb.*) *sphaeroides* (Allen et al., 1987; Deisenhofer et al., 1985) are available. However, in native membranes, the RC forms an integral part of the core complex (RC-LH1), the structure of which is known only at low resolution. Data acquired by cryo electron microscopy (EM), AFM and X-ray diffraction, of core complexes of several species, show the LH1 assembly around the RC can have several different architectures: in *Rsp. rubrum* (Jamieson et al., 2002), *Rsp. photometricum* (Scheuring and Sturgis, 2005), and *Blc. viridis* (Scheuring et al., 2003), an apparently closed elliptical assembly of 16 LH1 subunits surrounds the RC. In *Rps. palustris* (Roszak et al., 2003), the RC is surrounded by an elliptical assembly of 15 LH1 subunits and 1 W-subunit. In *Rb. blasticus* (Scheuring et al., 2005) and *Rb. sphaeroides* (Qian et al., 2005), the cores form S-shaped assemblies containing 2 RC, 26 or 28 LH1, and 2 PufX polypeptides. The detailed structure of *Rhodobacter* core complexes is still matter of some debate (Qian et al., 2005; Scheuring et al., 2005). The high-resolution X-ray structures of the cytochrome bc_1 complex (Berry et al., 2004), and the F_1 (Stock et al., 1999) and F_O (Meier et al., 2005) parts of the ATP synthase are equally available.

The atomic force microscope (AFM) (Binnig et al., 1986), with it's high signal-to-noise ratio, has recently produced the first images at high resolution giving insights into the architecture of the photosynthetic apparatus in different bacteria: *Blc. viridis* (Scheuring et al., 2003), *Rsp. photometricum* (Scheuring and Sturgis, 2005; Scheuring et al., 2004a,b), *Rb. sphaeroides* (Bahatyrova et al., 2004), and *Rb. blasticus* (Scheuring et al., 2005). While membranes of *Blc. viridis* and *Rb. blasticus* were pretreated by freeze–thaw cycles, and *Rb. sphaeroides* membranes by detergent treatment, only the studies on *Rsp. photometricum* were made on completely native chromatophores. In *Rsp. photometricum* membranes, two different types of membrane areas were identified: domains containing hexagonal packed nonameric LH2, and domains containing a disorganized fixed composition mixture of core complexes and LH2 antennae (Scheuring and Sturgis, 2005).

This AFM analysis on chromatophores of *Phsp. molischianum* is the second study performed on untreated native photosynthetic membranes. Structural data on single molecules and on their assembly in the native membranes were obtained. The RC is found to be fully enclosed by an elliptic LH1 assembly. As expected an octameric LH2 was found. However, some individual LH2 differ significantly in ring diameter indicating variations in stoichiometry around the general octameric assembly. From our images on native membranes and the LH2 structure of *Phsp. molischianum* (Koepke et al., 1996), we can deduce the pigment distances between neighboring complexes, shedding light on energy transfer pathways and properties in *Phsp. molischianum*. Surprisingly, LH2 octamers form hexagonally packed antenna domains suggesting that solvation effects rather than specific protein–protein interactions drive assembly.

2. Results and discussion

2.1. Phsp. molischianum chromatophore characterization

Phaeospirillum (*Phsp.*) *molischianum* cells were grown anaerobically and photoheterotrophically. In EM thin section of *Phsp. molischianum* cells, photosynthetic intracytoplasmic membranes (ICM) are visible as stacked invaginations of the cytoplasmic membrane, easily identified as dark lines inside the bacteria with sizes ranging from 100 to 500 nm (Fig. 1A; inset), varying with bacteria and growth conditions. These stacked ICM contain the membrane proteins of the photosynthetic machinery (Gibbs et al., 1965). UV-visible-near-IR absorption spectra of these chromatophores (Fig. 1A) document primarily the presence of the following protein–pigment complexes of the photosynthetic system: bc_1 complex, RC, LH1, and LH2. The LH2/core-complex ratio is calculated to be >4 (Fig. 1B), though this calculation is made difficult in this species by the possible presence of a B800–820 antenna. ICM preparations contain double bilayer membrane fragments of fairly homogeneous size as analyzed by EM (Fig. 1C) and AFM (Fig. 1E). These fragments have a fairly heterogeneous thickness of ~20 nm measured in AFM overview topographs, indicating two bilayers stacked to each other with the upper relative loosely attached. The fragment size distributions were similar in both EM (Fig. 1D; $n = 580$) and AFM (Fig. 1F; $n = 105$) analysis: fragments with size of ~110 nm were imaged by AFM, suggesting little size related selection during adsorption on the mica surface for AFM.

2.2. Architecture of the photosynthetic apparatus

AFM imaging at molecular resolution allows analysis of the photosynthetic apparatus assembly in chromatophore fragments of *Phsp. molischianum* (Fig. 2). As in previous studies the proteins of the photosynthetic apparatus show a strong tendency to cluster (Scheuring et al., 2004a). All photosynthetic proteins are in physical contact assuring efficient energy transfer between the pigment molecules within and between the complexes (Scheuring et al., 2004a). As can be seen (Figs. 2A–E), a wide variety of protein arrangements exist. About 30% of core complexes are completely surrounded by LH2. For steric reasons core complexes have a total of 7 nearest neighbors, evidence that the models previously reported (Hu et al., 2002; Papiz et al., 1996), in which the core complex is surrounded by 8 LH2 at equal distance, are too densely packed. About 70% of the core complexes are connected to other cores (Fig. 2G). This reflects an effort to maximize the efficiency of the photosynthetic machinery. Energy transfer reactions are much faster (LH2–LH2: 10 ps; LH2–LH1: 3–8 ps; LH1-RC: 16–25 ps (Hu et al., 2002)) than the reduction of the RC. The observed arrangement with core–core contacts is probably important for the function of this photosynthetic apparatus in realistic conditions where photons are abundant and represents a compromise between maximal trapping and maximal core connectivity. Such

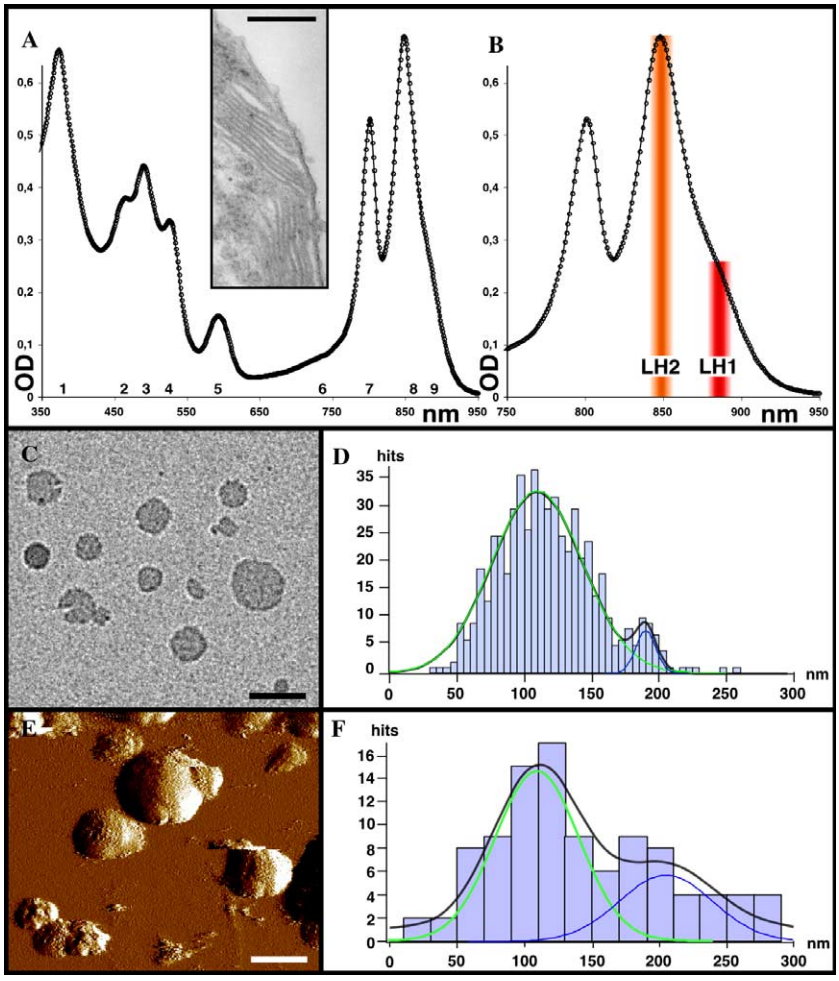

Fig. 1. Characterization of *Phsp. molischianum* intracytoplasmic membranes (ICM). (A) Absorption spectrum of *Phsp. molischianum* chromatophores. Peaks correspond to: (1) BChl B_x and B_y at 376 nm; (2–4) carotenoid S_0 at 460, 488, and 528 nm; (5) LH2/LH1/RC (Q_x) at 592 nm; (6) RC (Bpheo) at 760 nm; (7) LH2 (Q_y) with underlying RC (Bchl) at 796 nm; (8) LH2 (Q_y) at 848 nm; and (9) LH1 (Q_y) at 884 nm. Inset: EM thin section of *Phsp. molischianum* cell with stacked ICM with sizes ranging from 100 to 500 nm in section (scale bar: 250 nm). (B) The absorption ratio LH2 (848 nm)/LH1 (884 nm) is ~2.5 corresponding to a LH2 ring/core-complex ratio >4. (C) EM overview micrograph of native chromatophores (scale bar: 200 nm). (D) Size histogram of native chromatophores calculated from overview EM data ($n = 580$). The histogram is well fitted by the sum (black line) of two Gaussians peaking at 110 nm (green line) and 190 nm (blue line) with widths of 48 and 10 nm, respectively. (E) AFM overview topograph of native chromatophores (scale bar: 200 nm). (F) Size histogram of native chromatophores calculated from AFM data ($n = 105$). The histogram is well fitted by the sum (black line) of two Gaussians peaking at 108 nm (green line) and 193 nm (blue line) with widths of 41 and 29 nm, respectively.

connectivity allows an exciton to search for an 'open' RC. The irregular complex arrangement with preferential associations is strongly reminiscent of that found in *Rsp. photometricum* (Scheuring et al., 2004a), and different from the supramolecular architectures found in *Blc. viridis* (Scheuring et al., 2003), *Rb. sphaeroides* (Bahatyrova et al., 2004), and *Rb. blasticus* (Scheuring et al., 2005). Importantly, this analysis of the supramolecular architecture of the photosynthetic complexes in *Phsp. molischianum* chromatophores represents the second study on non-fused membrane fragments, comparable to the analysis of *Rsp. photometricum* membranes (Scheuring and Sturgis, 2005; Scheuring et al., 2004a,b). Surprisingly, despite the structural differences between individual proteins, the *Phsp. molischianum* LH2 complex is an octamer (Koepke et al., 1996), unlike that of *Rsp. photometricum* which is a nonamer, the overall supramolecular protein arrangement is similar in *Rsp. photometricum* and *Phsp. molischianum*. In both species, proteins are densely packed in the membranes, core complexes are monomeric but cluster, and large antenna domains formed by para-crystalline LH2 are found. In contrast the *Rhodobacter* strains, *Rb. sphaeroides* (Bahatyrova et al., 2004) and *Rb. blasticus* (Scheuring et al., 2005) have core complexes that are structural dimers due to the presence of PufX. Such dimerization could be functionally related to the clustering of the core complexes found in *Rsp. photometricum* and *Phsp. molischianum* assuring RC connectivity. Furthermore, in *Rhodobacter* core complexes, the LH1 rings have ~25 Å 'gaps' evidenced as quinone/quinol gates (Scheuring et al., 2005), whereas in *Rsp. photometricum* and *Phsp. molischianum*, the LH1 ring was found to completely enclose the RC. Finally, in *Blc. viridis*, a strain that lacks LH2, the supramolecular arrangement of

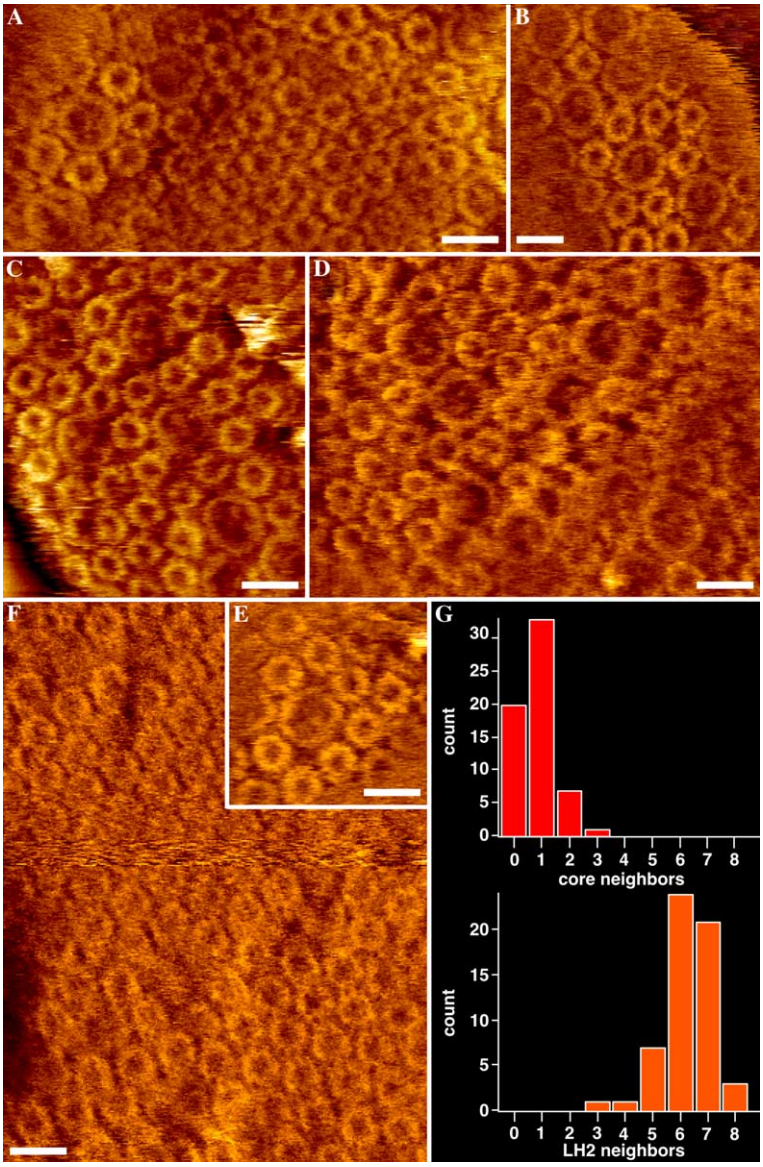

Fig. 2. AFM analysis of the protein assembly in native photosynthetic membranes of *Phsp. molischianum*. (A–E) AFM topographs of core complex containing membrane domains. A wide variety of complex assemblies are found (scale bar: 10 nm; color scale: 5 nm). (F) Antenna domain constituted of hexagonal para-crystalline LH2. (G) Histograms of adjacent molecules to a core complex (top: core-complex neighbors; bottom: LH2 neighbors). The diagrams report the variety of assemblies in the chromatophores ($n = 58$). About 70% of the core complexes are connected with other cores.

the photosynthetic complexes can hardly be compared to that of these LH2-containing species. Hence, many different supramolecular arrangements of the photosynthetic complexes permit efficient photosynthetic growth and represent most probably adaptation to the particular environmental conditions of the different species.

An interesting 'negative' result is that the cytochrome bc_1 complex and the ATP synthase could not be seen in our images. Studies on photosynthetic membranes have now been performed on five different bacteria: *Blc. viridis* (Scheuring et al., 2003), *Rsp. photometricum* (Scheuring et al., 2004a), *Rb. sphaeroides* (Bahatyrova et al., 2004), *Rb. blasticus* (Scheuring et al., 2005), and *Phsp. molischianum* (this study). Significantly, while these different species reveal different supramolecular organization of LH2 and core complexes, the cytochrome bc_1 complex or the ATP synthase have never been observed. It thus seems safe to affirm that in many bacteria large areas of photosynthetic membranes do not contain any of either of these two membrane proteins. This is clearly paradoxical as these proteins are essential for photosynthetic activity. However, these two complexes also play a role in other respiratory pathways such as oxidative phosphorylation as complexes IV and V, suggesting that for rapid physiological adaptation their localization may be in between photosynthetically active and respiratory chain membrane domains.

2.3. Structural analysis of photosynthetic complexes

Several high-resolution images (Fig. 2) allow the calculation of averages of the photosynthetic complexes using

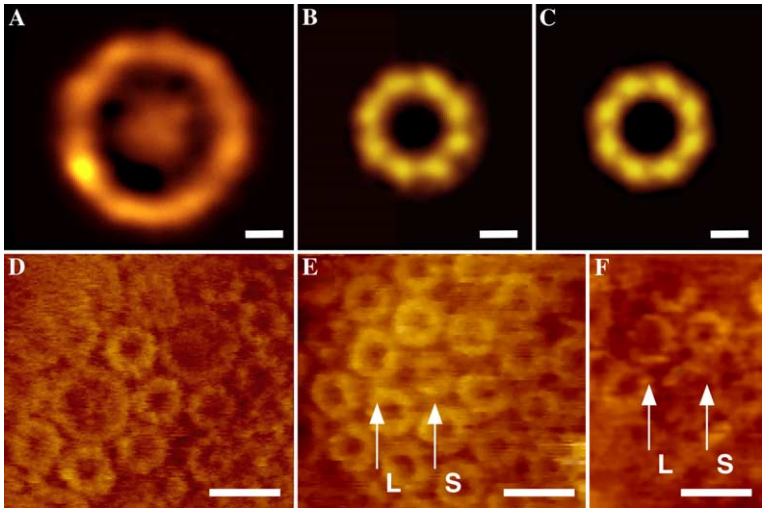

Fig. 3. Structural analysis of the complexes found in native photosynthetic membranes of *Phsp. molischianum*. (A) Core-complex average ($n = 151$; scale bar: 20 Å; color scale: 1 nm): the RC is completely surrounded by an elliptical LH1 assembly with long and short axes of 95 and 85 Å. (B) Image of two individual core complexes (scale bar 10 nm). In both differently oriented core complexes, the LH1 assembly forms a closed ellipsis. (C) LH2 complex average ($n = 511$; scale bar: 20 Å; color scale: 1 nm). The LH2 complex is octameric with a top ring diameter of 48 Å. (D) 8-fold symmetrized LH2 average (scale bar: 20 Å; color scale: 1 nm). The subunits reveal a slight left-handed twist. (E and F) Besides the majority of LH2 complexes that favorably compare with the 8-fold LH2 average, some LH2 rings appear smaller (S) with diameters ~38 Å or larger (L) with diameters up to 57 Å (scale bar: 10 nm, color scale: 1 nm).

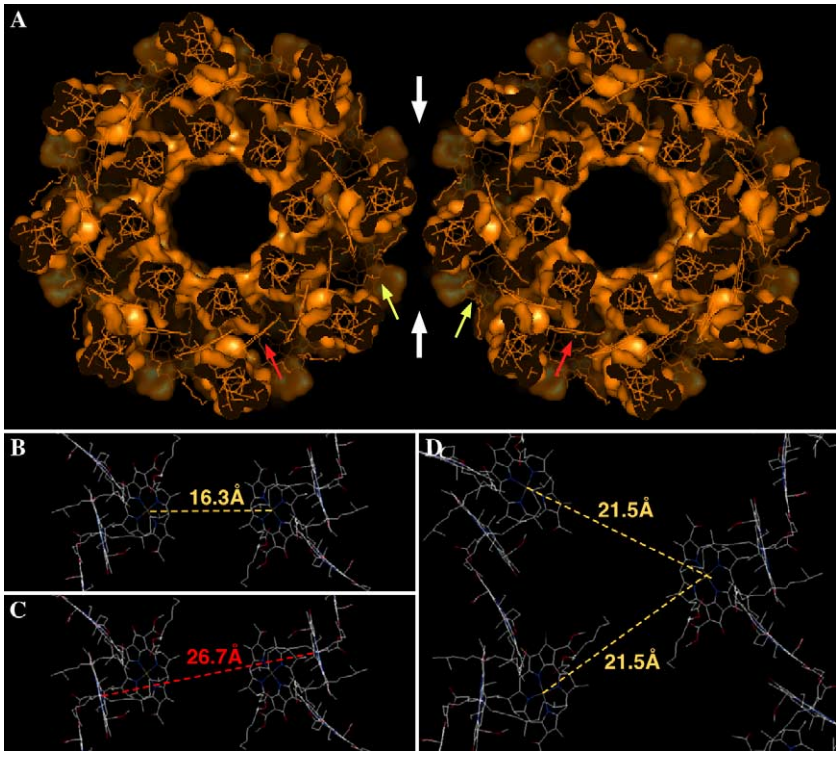

Fig. 4. Distances between BChls between LH2 in antenna domains of *Phsp. molischianum.* Based on the X-ray structure of *Phsp. molischianum* LH2 (Koepke et al., 1996) and the measured LH2–LH2 center-to-center distance of 74 Å, the inter-complex pigment distances are measured. The distances within the LH2 were extensively studied: B800–B800: 22.0 Å; B850a–B850a: 9.3 Å; B850a–B850b: 8.9 Å. (A) Structure and molecular surface representation of two LH2 rings. The structure is sliced slightly above the B850 pigment ring (red arrows). Further down in space the B800 pigments can be seen (yellow arrows). There is no space for lipid molecules at the interface between the two rings (white arrows). (B) Depending on LH2 ring rotation B800–B800 distances can be as short as 16.3 Å. (C) Depending on LH2 ring rotation B850–B850 distances vary only little between 26.7 and 28.3 Å, assuring efficient energy transfer. (D) Depending on LH2 ring rotation B800–B800 distances up to 21.5 Å are found.

reference free single particle alignment procedures. An elliptic LH1 assembly, with long and short axes of 95 ± 3 Å and 85 ± 3 Å ($n = 151$; measured on protrusion top), surrounds the RC. This size and shape for the core complex is very similar to that found for *Rsp. photometricum* [top axes distances: 99 Å and 83 Å (Scheuring and Sturgis, 2005)],

Rsp. rubrum [outer diameters: 115 Å and 105 Å (Jamieson et al., 2002)], and *Rps. palustris* [distances between β-polypeptide helixes: 110 Å and 95 Å (Roszak et al., 2003)]. LH1 fences surround the RC completely, as documented by raw data images (Figs. 2B and 3B), hence, although not all individual LH1 subunits could be resolved, we suspect that 16 LH1 subunits are present as in *Blc. viridis* (Scheuring et al., 2003), *Rsp. rubrum* (Jamieson et al., 2002), and *Rsp. photometricum* (Scheuring and Sturgis, 2005). The LH1 subunits protrude by 9 ± 2 Å ($n = 15$). The relative loss of topographical features in the average (Fig. 3A), compared to raw data images (Figs. 3B and 2), is attributed to LH1 flexibility, and thus variability of the images averaged.

Averaging of the LH2 rings significantly increased the signal-to-noise ratio. Most LH2 could be aligned and averaged to give a ring shaped assembly with 8-fold symmetry and a top ring diameter of 48 Å. The subunits of the LH2 protrude by 10 ± 2 Å ($n = 23$). Structural analysis of LH2 by X-ray diffraction, EM and AFM revealed 9 subunits in *Rps. acidophila* (Gonçalves et al., 2005; McDermott et al., 1995), *Rb. sphaeroides* (Walz et al., 1998), *Rubrivivax* (*Rvi.*) *gelatinosus* (Scheuring et al., 2001), *Rsp. photometricum* (Scheuring and Sturgis, 2005; Scheuring et al., 2004a), and *Rhodovulum sulfidophilum* (Montoya et al., 1995). Consistent with our data on native chromatophores, the X-ray structure of *Phsp. molischianum* has 8 subunits (Koepke et al., 1996). However, in native membranes some LH2 revealed size variability (Figs. 3E and F), most obviously some individual complexes differ by ~20% from the normal diameter (48 Å) with diameters ranging from ~38 Å (arrow S, small) to ~57 Å (arrow L, large). These smaller and larger LH2 are located side by side with "normal" LH2 and are not affected in the overall circular arrangement of the subunits. Such variability of LH2 size has previously been shown by high-resolution AFM of native chromatophores of *Rsp. photometricum* to result from variability in subunit stoichiometry and to go hand in hand with slight absorption shift (Scheuring et al., 2004a). Interestingly, theoretical studies calculating the free energy potentials indicate angular freedom of interaction of a few degrees between LH2 subunits of *Phsp. molischianum* (Janosi et al., 2005), which could result in size heterogeneity. LH2 stoichiometry variability could represent a strategy for broader light absorption and/or a strategy for optimizing packing in a heterogeneous membrane or an inevitable accident of assembly.

2.4. Energy transfer

Close packing of photosynthetic complexes in native membranes is directly related to the energy transfer. Pigment molecules within antenna complexes need to be at distances ~30 Å from each other to assure efficient energy transfer (Hu et al., 2002). LH2–LH2 distances in native membranes are 74 ± 1 Å ($n = 36$; Fig. 4A). Using the atomic coordinates (Koepke et al., 1996), we can evaluate the inter-complex pigment–pigment distances (measured between central Mg^{2+} atoms). Depending on the relative rotation of the neighboring complexes, the distances vary between 16.3 Å (Fig. 4B) and 21.5 Å (Fig. 4D) for B800, and 26.7 Å (Fig. 4C) and 28.3 Å for B850. It is interesting to note that the inter-complex B800–B800 distances are shorter than the intra-complex ones (22.0 Å).

2.5. LH2 antenna packing

An unexpected observation is that octameric LH2 forms hexagonal arrays in native membranes (Fig. 2F), like nonameric LH2 in chromatophores of *Rsp. photometricum* (Scheuring and Sturgis, 2005). Octameric LH2 has a symmetry mismatch with a hexagonal lattice and a symmetry match with a square lattice. LH2 8-mers can be packed in a square lattice with 4 optimized nearest neighbor contacts with adjacent LH2 and a packing density of 0.785. In a hexagonal lattice the density is higher (0.907) but maximally only 2 optimized contacts with neighboring LH2 can be formed. In contrast, nonameric LH2 is in better symmetry match in a hexagonal lattice than in a square lattice. LH2 9-mers gain higher packing density in a hexagonal lattice and the possibility to form an average of 2 optimized contacts, versus lower density and maximally only 1 optimized contact in a square lattice.

In this context, many native 2D-lattices form hexagonal or square assemblies following the molecular symmetry of the molecules involved due to the formation of specific inter-molecular contacts. The hexameric uroplakin particles in the bladder membrane form hexagonal lattices (Min et al., 2003). The bacteriorhodopsin trimers are inserted in a hexagonal lattice with three equal and specific inter-molecular interactions in the native purple membrane (Henderson et al., 1990). Tetrameric aquaporins 0 and 4 form native square lattices in cell membranes (Furman et al., 2003; Gonen et al., 2004). S-layers, a paradigm of self-assembly systems, form square or hexagonal lattices depending on whether the core assembly is a tetramer or a hexamer (Hoiczyk and Baumeister, 1995; Sara and Sleytr, 1994). In all these native self-assembled 2D-lattices specific inter-molecular contacts are formed. Here, in striking contrast, we observe a packing that does not follow the inherent molecular symmetry.

The observation that both 8-fold (*Phsp. molischianum*; this work) and 9-fold (*Rsp. photometricum*; Scheuring and Sturgis, 2005) LH2 form hexagonal antenna domains, while 8-fold LH2 could double the optimized protein–protein contacts in a square lattice, is strong evidence that high packing density is favored over specific protein–protein contacts. This suggests that lipo-phobic effects, e.g., a solvation mismatch between the membrane protein and the lipid bilayer, drive complex assembly. Such an effect could result from hydrophobic mismatch (Mouritsen and Bloom, 1984), or a solvation incompatibility between the branched polyprenoid chains exposed by LH2 and the anisotropic linear aliphatic chains of the

phospholipids. The resulting packing with LH2–LH2 distances of 74 Å is so dense that there are no lipid molecules intercalated between complexes (Fig. 4A, white arrows).

This report provides further information on the bacterial photosynthetic apparatus. It is the second report on native non-fused membranes of purple bacteria and brings novel insight into multi-protein assemblies in cell membranes. The function of the assembled system is directly related to their organization and the relative position of the different components in the membrane. After the description of the function of individual proteins that has evolved along with high-resolution structural analysis, a higher level of understanding of their interactions in complicated machineries is needed. Some of the most important functions in nature are multi-protein systems such as respiration, photosynthesis, and signal transduction. AFM is a unique tool to study such systems, and will provide in situ information that complements functional data and structures of individual complexes.

3. Materials and methods

3.1. Membrane preparation

Phsp. molischianum cells, strain DSM 120, were grown anaerobically and photoheterotrophically, and harvested in late log phase. Cells were broken by a single passage through a French pressure cell. Lysates were loaded directly onto 5–60% sucrose gradients and centrifuged. ICM sedimented at about 40% sucrose. The membranes were dialyzed against a sucrose free buffer before AFM analysis.

3.2. Atomic force microscopy

Mica prepared as described (Schabert and Engel, 1994) was freshly cleaved and used as the support. Three microliters of membrane solution were injected into the 40 µl adsorption buffer (10 mM Tris–HCl, pH 7.2, 150 mM KCl, 25 mM $MgCl_2$). After ~1 h, the sample was rinsed with recording buffer (10 mM Tris–HCl, pH 7.2, 150 mM KCl). Imaging was performed with a commercial Nanoscope-E AFM (Veeco, Santa Barbara, CA, USA) equipped with a 160 µm scanner (J-scanner) and oxide-sharpened Si_3N_4 cantilevers (length 100 µm; $k = 0.09$ N/m; Olympus Ltd., Tokyo, Japan). For imaging minimal loading forces of ~100 pN were applied, at scan frequencies of 4–7 Hz using optimized feedback parameters.

3.3. Data analysis

Averages of complexes were calculated using Xmipp single particle analysis package and reference free alignment procedures (Marabini et al., 1996). Pymol and Swiss-pdbViewer were used to create Fig. 4. Igor software was used for all other data analysis.

Acknowledgments

We thank Dr J.L. Rigaud for constant support and V. Prima for technical assistance. This study was supported by the Ministère de la l'Education Nationale (R.P.G.), the INSERM (S.S.), the CNRS (J.S.), and an 'ACI Nanosciences 2004' grant (NR206).

References

Allen, J.P., Feher, G., Yeates, T.O., Komiya, H., Rees, D.C., 1987. Structure of the reaction center from *Rhodobacter sphaeroides* R-26: the protein subunits. Proc. Natl. Acad. Sci. USA 84, 6162–6166.

Bahatyrova, S., Frese, R.N., Siebert, C.A., Olsen, J.D., Van Der Werf, K.O., van Grondelle, R., Niederman, R.A., Bullough, P.A., Otto, C., Hunter, C.N., 2004. The native architecture of a photosynthetic membrane. Nature 430, 1058–1062.

Berry, E.A., Huang, L.-S., Saechao, L.K., Pon, N.G., Valkova-Valchanova, M., Daldal, F., 2004. X-ray structure of *Rhodobacter capsulatus* cytochrome bc1: comparison with its mitochondrial and chloroplast counterparts. Photosynth. Res. 81, 251–275.

Binnig, G., Quate, C.F., Gerber, C., 1986. Atomic force microscope. Phys. Rev. Lett. 56, 930–933.

Deisenhofer, J., Epp, O., Miki, K., Huber, R., Michel, H., 1985. Structure of the protein subunits in the photosynthetic reaction centre of *Rhodopseudomonas viridis* at 3 Å resolution. Nature 318, 618–624.

Furman, C.S., Gorelick-Feldman, D.A., Davidson, K.G., Yasumura, T., Neely, J.D., Agre, P., Rash, J.E., 2003. Aquaporin-4 square array assembly: opposing actions of M1 and M23 isoforms. Proc. Natl. Acad. Sci. USA 100, 13609–13614.

Gibbs, S.P., Sistrom, W.R., Worden, P.B., 1965. The photosynthetic apparatus of *Rhodospirillum molischianum*. J. Cell Biol. 26, 395–412.

Gonçalves, R.P., Busselez, J., Lévy, D., Seguin, J., Scheuring, S., 2005. Membrane insertion of *Rhodopseudomonas acidophila* light harvesting complex 2 (LH2) investigated by high resolution AFM. J. Struct. Biol. 149, 79–86.

Gonen, T., Sliz, P., Kistler, J., Cheng, Y., Walz, T., 2004. Aquaporin-0 membrane junctions reveal the structure of a closed water pore. Nature 13, 193–197.

Henderson, R., Baldwin, J.M., Ceska, T.A., Zemlin, F., Beckman, E., Downing, K.H., 1990. Model for the structure of bacteriorhodopsin based on high-resolution electron cryo-microscopy. J. Mol. Biol. 213, 899–929.

Hoiczyk, E., Baumeister, W., 1995. Envelope structure of four gliding filamentous cyanobacteria. J. Bacteriol. 177, 2387–2395.

Hu, X., Ritz, T., Damjanovic, A., Autenrieth, F., Schulten, K., 2002. Photosynthetic apparatus of purple bacteria. Quart. Rev. Biophys. 35, 1–62.

Jamieson, S.J., Wang, P., Qian, P., Kirkland, J.Y., Conroy, M.J., Hunter, C.N., Bullough, P.A., 2002. Projection structure of the photosynthetic reaction centre-antenna complex of *Rhodospirillum rubrum* at 8.5 Å resolution. EMBO J. 21, 3927–3935.

Janosi, L., Keer, H., Kosztin, I., Ritz, T., 2005. Influence of subunit structure on the oligomerization state of light harvesting complexes: a free energy calculation study. Chem. Phys arXiv:physics/0504213.

Koepke, J., Hu, X., Muenke, C., Schulten, K., Michel, H., 1996. The crystal structure of the light-harvesting complex II (B800–850) from *Rhodospirillum molischianum*. Structure 4, 581–597.

Marabini, R., Masegosa, I.M., San Martin, C., Marco, S., Fernandez, J.J., de la Fraga, C.G., Carazo, J.M., 1996. Xmipp: an image processing package for electron microscopy. J. Struct. Biol. 116, 237–240.

McDermott, G., Prince, S.M., Freer, A.A., Hawthornthwaite-Lawless, A.M., Papiz, M.Z., Cogdell, R.J., Isaacs, N.W., 1995. Crystal structure of an integral membrane light-harvesting complex from photosynthetic bacteria. Nature 374, 517–521.

Meier, T., Polzer, P., Diederichs, K., Welte, W., Dimroth, P., 2005. Structure of the rotor ring of F-type Na^+-ATPase from *Ilyobacter tartaricus*. Science 308, 659–662.

Min, G., Zhou, G., Schapira, M., Sun, T.T., Kong, X.P., 2003. Structural basis of urothelial permeability barrier function as revealed by cryo-EM studies of the 16 nm uroplakin particle. J. Cell Sci. 116, 4087–4094.

Montoya, G., Cyrklaff, M., Sinning, I., 1995. Two-dimensional crystallization and preliminary structure analysis of light harvesting II (B800–850) complex from the purple bacterium *Rhodovulum sulfidophilum*. J. Mol. Biol. 250, 1–10.

Mouritsen, O.G., Bloom, M., 1984. Mattress model of lipid–protein interactions in membranes. Biophys. J. 46, 141–153.

Papiz, M.Z., Prince, S.M., Hawthornthwaite-Lawless, A.M., McDermott, G., Freer, A.A., Isaacs, N.W., Cogdell, R.J., 1996. A model for the photosynthetic apparatus of purple bacteria. Trends Plant Sci. 1, 198–206.

Papiz, M.Z., Prince, S.M., Howard, T.D., Cogdell, R.J., Isaacs, N.W., 2003. The structure and thermal motion of the B800–850 LH2 complex from *Rps. acidophila* at 2.0 Å resolution and 100K: new structural features and functionally relevant motions. J. Mol. Biol. 326, 1523–1538.

Qian, P., Hunter, C.N., Bullough, P.A., 2005. The 8.5 Å projection structure of the Core RC-LH1-PufX dimer of *Rhodobacter sphaeroides*. J. Mol. Biol. 349, 948–960.

Roszak, A.W., Howard, T.D., Southall, J., Gardiner, A.T., Law, C.J., Isaacs, N.W., Cogdell, R.J., 2003. Crystal structure of the RC-LH1 core complex from *Rhodopseudomonas palustris*. Science 302, 1969–1972.

Sara, M., Sleytr, U.B., 1994. Comparative studies of S-layer proteins from *Bacillus stearothermophilus* strains expressed during growth in continuous culture under oxygen-limited and non-oxygen-limited conditions. J. Bacteriol. 176, 7182–7189.

Schabert, F.A., Engel, A., 1994. Reproducible acquisition of *Escherichia coli* porin surface topographs by atomic force microscopy. Biophys. J. 67, 2394–2403.

Scheuring, S., Busselez, J., Lévy, D., 2005. Structure of the dimeric PufX-containing core complex of *Rhodobacter blasticus* by in situ AFM. J. Biol. Chem. 180, 1426–1431.

Scheuring, S., Reiss-Husson, F., Engel, A., Rigaud, J.-L., Ranck, J.-L., 2001. High resolution topographs of the *Rubrivivax gelatinosus* light-harvesting complex 2. EMBO J. 20, 3029–3035.

Scheuring, S., Rigaud, J.-L., Sturgis, J.N., 2004a. Variable LH2 stoichiometry and core clustering in native membranes of *Rhodospirillum photometricum*. EMBO J. 23, 4127–4133.

Scheuring, S., Seguin, J., Marco, S., Lévy, D., Robert, B., Rigaud, J.L., 2003. Nanodissection and high-resolution imaging of the *Rhodopseudomonas viridis* photosynthetic core-complex in native membranes by AFM. Proc. Natl. Acad. Sci. USA 100, 1690–1693.

Scheuring, S., Sturgis, J.N., 2005. Chromatic adaptation of photosynthetic membranes. Science 309, 484–487.

Scheuring, S., Sturgis, J.N., Prima, V., Bernadac, A., Lévy, D., Rigaud, J.-L., 2004b. Watching the photosynthetic apparatus in native membranes. Proc. Natl. Acad. Sci. USA 101, 11293–11297.

Stock, D., Leslie, A.G., Walker, J.E., 1999. Molecular architecture of the rotary motor in ATP synthase. Science 286, 1700–1705.

Walz, T., Jamieson, S.J., Bowers, C.M., Bullough, P.A., Hunter, C.N., 1998. Projection structures of three photosynthetic complexes from *Rhodobacter sphaeroides*: LH2 at 6 Å, LH1 and RC-LH1 at 25 Å. J. Mol. Biol. 282, 833–845.